Back-to-Back Inclusive Dijets in Deep Inelastic Scattering at Small x: Complete NLO Results and Predictions

Paul Caucal,[1,*] Farid Salazar,[2,3,4,5,†] Björn Schenke,[6,‡] Tomasz Stebel,[7,§] and Raju Venugopalan[6,∥]

[1]*SUBATECH UMR 6457, IMT Atlantique, Université de Nantes, IN2P3/CNRS, 4 rue Alfred Kastler, 44307 Nantes, France*
[2]*Lawrence Berkeley National Laboratory, Nuclear Science Division, Berkeley, California 94720, USA*
[3]*Physics Department, University of California, Berkeley, California 94720, USA*
[4]*Department of Physics and Astronomy, University of California, Los Angeles, California 90095, USA*
[5]*Mani L. Bhaumik Institute for Theoretical Physics, University of California, Los Angeles, California 90095, USA*
[6]*Physics Department, Brookhaven National Laboratory, Upton, New York 11973, USA*
[7]*Institute of Theoretical Physics, Jagiellonian University, ulica Lojasiewicza 11, 30-348 Kraków, Poland*

(Received 12 August 2023; revised 16 January 2024; accepted 30 January 2024; published 20 February 2024)

We compute the back-to-back dijet cross section in deep inelastic scattering at small x to next-to-leading order (NLO) in the color glass condensate effective field theory. Our result can be factorized into a convolution of the Weizsäcker-Williams gluon transverse-momentum-dependent distribution function (WW gluon TMD) with a universal soft factor and an NLO coefficient function. The soft factor includes both double and single logarithms in the ratio of the relative transverse momentum $P_\perp$ of the dijet pair to the dijet momentum imbalance $q_\perp$; its renormalization group (RG) evolution is resummed into the Sudakov factor. Likewise, the WW TMD obeys a nonlinear RG equation in x that is kinematically constrained to satisfy both the lifetime and rapidity ordering of the projectile. Exact analytical expressions are obtained for the NLO coefficient function of transversely and longitudinally polarized photons. Our results allow for the first quantitative separation of the dynamics of Sudakov suppression from that of gluon saturation. They can be extended to other final states and provide a framework for precision tests of novel QCD many-body dynamics at the Electron-Ion Collider.

DOI: 10.1103/PhysRevLett.132.081902

The transverse-momentum-dependent gluon Weizsäcker-Williams distribution (WW TMD) is an object of fundamental interest in QCD [1]. A particularly interesting feature is the prediction [2–4] that, in contrast to the WW photon distribution in QED, strong nonlinear gluon self-interactions in QCD at small x saturate its growth for transverse momenta $k_\perp \lesssim Q_s$, where $Q_s(x)$ is an emergent saturation scale [5,6].

A golden channel to extract the WW TMD is the inclusive measurement of back-to-back jets (or hadrons) in deeply inelastic electron-nucleus scattering ($e + A$ DIS) [7,8], characterized by the relative transverse momentum $P_\perp$ of the dijet pair and the dijet momentum imbalance $q_\perp$. For clean extraction of this quantity, perturbative QCD (pQCD) requires that $P_\perp \gg q_\perp \gg \Lambda_{\rm QCD}$, where $\Lambda_{\rm QCD}$ is the intrinsic QCD scale. At leading order (LO), this process factorizes into the product of a hard factor computed in pQCD and the nonperturbative gluon WW TMD [8]. At next-to-leading order (NLO) in the QCD coupling α_s, the mismatch between real and virtual soft gluon radiation leads to $\alpha_s \ln^2(P_\perp/q_\perp)$ contributions that significantly suppress the back-to-back cross section for $P_\perp \gg q_\perp$ [9–17]. NLO effects in gluon radiation also generate large small-x logarithms that drive gluon saturation [15–17]. It is therefore critical to understand the interplay of these effects in the extraction of the WW gluon TMD.

In this Letter, we will demonstrate within the framework of the color glass condensate effective field theory (CGC EFT) [18–20] that TMD factorization of the inclusive back-to-back dijet cross section in DIS at small x persists at NLO [21]. Our derivation is valid to leading power (LP) in $q_\perp/P_\perp$, $Q_s/P_\perp$, and to all orders in $Q_s/q_\perp$. We identify three key components that emerge from our NLO calculation: (i) The WW gluon TMD, satisfying a nonlinear renormalization group evolution equation (RGE) in x that incorporates the dynamics of gluon saturation, (ii) double and single Sudakov logarithms of $P_\perp/q_\perp$, and (iii) perturbative hard factors (functions of $P_\perp$ and the photon virtuality Q^2).

We will apply our results to the kinematics of the future Electron-Ion Collider (EIC) [23–25]. While dijet studies are challenging at small x [26–31], a window in the required phase space may exist for this theoretically robust final

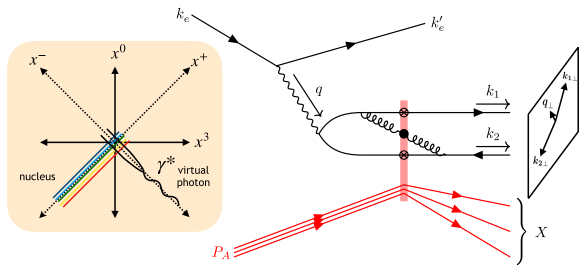

FIG. 1. NLO DIS diagram for dijet production in dipole scattering off shock wave (red rectangle) in the CGC EFT. The nuclear target and the virtual photon move close to the light cone with large q^- and P_A^+ components, respectively.

state. The extension of our study to the phenomenologically more accessible [32], if theoretically less robust, dihadron final state is straightforward [33]. Our computation is the first to include all above listed NLO components to determine the relative impact of Sudakov suppression and gluon saturation.

In the dipole frame with virtual photon four-momentum $q^\mu = (-Q^2/(2q^-), q^-, \mathbf{0}_\perp)$ and nucleon four-momentum $P^\mu = (P^+, 0, \mathbf{0}_\perp)$, the inclusive LO dijet cross section $d\sigma_{\rm LO}^\lambda = z_1 z_2 (d\sigma_{\rm LO}^\lambda / d^2\boldsymbol{P}_\perp d^2\boldsymbol{q}_\perp dz_1 dz_2)$ can be expressed as [8,34]

$$\langle d\sigma_{\rm LO}^\lambda\rangle = \int d^2\boldsymbol{r}_\perp d^2\boldsymbol{r}'_\perp d^2\boldsymbol{b}_\perp d^2\boldsymbol{b}'_\perp e^{-i\boldsymbol{P}_\perp\cdot(\boldsymbol{r}_\perp - \boldsymbol{r}'_\perp)} \times e^{-i\boldsymbol{q}_\perp\cdot(\boldsymbol{b}_\perp-\boldsymbol{b}'_\perp)} \mathcal{R}^\lambda(\boldsymbol{r}_\perp, \boldsymbol{r}'_\perp)\langle \Xi(\boldsymbol{r}_\perp, \boldsymbol{r}'_\perp, \boldsymbol{b}_\perp, \boldsymbol{b}'_\perp)\rangle, \quad (1)$$

where $\lambda = L, T$ is the polarization of the photon, $\boldsymbol{P}_\perp = z_2 \boldsymbol{k}_{1\perp} - z_1 \boldsymbol{k}_{2\perp}$, $\boldsymbol{q}_\perp = \boldsymbol{k}_{1\perp} + \boldsymbol{k}_{2\perp}$, and $z_i = k_i^-/q^-$. Here $\mathcal{R}^\lambda$ is an analytic function representing the splitting of the virtual photon into the quark-antiquark dipole, and Ξ is an expression containing two-point dipole and four-point quadrupole lightlike Wilson line correlators. In the CGC EFT, these describe the coherent multiple scattering of the dipole with the nonperturbative shock wave classical gauge field configurations of the nuclear target; the $\langle \ldots \rangle$ is the average over static large-x color charge densities generating these configurations.

The one-loop (1L) correction to Eq. (1) consisting of real and virtual gluon emissions (with an example of the latter illustrated in Fig. 1) can be expressed as [34]

$$\alpha_s d\sigma_{\rm 1L}^\lambda = \alpha_s \int_{z_0}^1 \frac{dz_g}{z_g} \int d^2\boldsymbol{z}_\perp d\tilde{\sigma}_{\rm 1L}^\lambda(z_g, \boldsymbol{z}_\perp), \quad (2)$$

where $z_g = k_g^-/q^-$, k_g^- is the longitudinal momentum of the emitted (real or virtual) gluon, $\boldsymbol{z}_\perp$ is the transverse coordinate of the scattered gluon off the shock wave, and $z_0 \propto 1/s$ is a physical cutoff regulating the z_g divergence [34]. The integrand satisfies $\alpha_s \int_{\boldsymbol{z}_\perp} d\tilde{\sigma}_{\rm 1L}(0, \boldsymbol{z}_\perp) = H_{\rm LL} d\sigma_{\rm LO}$, with the leading log (LLx) Jalilian-Marian–Iancu–McLerran–Weigert–Leonidov–Kovner (JIMWLK) Hamiltonian of the form [35–41]

$$H_{\rm LL} = \frac{\alpha_s N_c}{2\pi^2} \int_{\boldsymbol{z}_\perp} \mathcal{K}_{\rm LL}, \quad (3)$$

where $\mathcal{K}_{\rm LL}$ is the LLx kernel. Equation (2) can be rewritten as

$$\alpha_s d\sigma_{\rm 1L}^\lambda = \ln\left(\frac{z_f}{z_0}\right) H_{\rm LL} d\sigma_{\rm LO}^\lambda + \alpha_s \int_0^1 \frac{dz_g}{z_g} \int d^2\boldsymbol{z}_\perp \times \left[d\tilde{\sigma}_{\rm 1L}^\lambda(z_g, \boldsymbol{z}_\perp) - d\tilde{\sigma}_{\rm 1L}^\lambda(0, \boldsymbol{z}_\perp)\Theta(z_f - z_g)\right]. \quad (4)$$

The first term isolates the large projectile-rapidity [42] logarithm by introducing an arbitrary $z_f \equiv k_f^-/q^-$ factorization scale separating "fast" gluons with $z_g \geq z_f$ from "slow" ones with $z_g \leq z_f$. Since the NLO cross section should be independent of z_f, the LO cross section satisfies the small-x JIMWLK RGE resumming $\alpha_s \ln(z_f/z_0)$ to all orders, which for $Y_f = \ln(z_f)$ is

$$\frac{\partial \langle d\sigma_{\rm LO}\rangle_{Y_f}}{\partial Y_f} = \langle H_{\rm LL} d\sigma_{\rm LO}\rangle_{Y_f}. \quad (5)$$

The second term in Eq. (4) constitutes the NLO impact factor $\langle d\sigma_{\rm NLO}\rangle_{Y_f}$. Here we have taken $z_0 \propto 1/s \to 0$; any dependence is power suppressed in the energy $\sqrt{s}$. At NLO, the Y_f dependence of the cross section is determined by the action of the next-to-leading log x (NLLx) JIMWLK Hamiltonian $H_{\rm LL} \to H_{\rm LL} + \alpha_s H_{\rm NLL}$ [43–46] on the LO cross section since the $\alpha_s^2 \ln(z_f/z_0)$ terms it resums are of the same order as $\langle d\sigma_{\rm NLO}\rangle_{Y_f}$.

We turn now to the back-to-back limit of the NLO inclusive dijet result in [34]. At LO, it was shown to have the TMD factorized form [8]

$$\langle d\sigma_{\rm LO}^{\lambda,\rm b2b}\rangle_{Y_0} = \mathcal{H}_{\rm LO}^{\lambda,ij} \int_{\boldsymbol{b}_\perp, \boldsymbol{b}'_\perp} \frac{e^{-i\boldsymbol{q}_\perp\cdot\boldsymbol{r}_{bb'}}}{(2\pi)^4} \hat{G}_{Y_0}^{ij}(\boldsymbol{r}_{bb'}, \mu), \quad (6)$$

with $\boldsymbol{r}_{bb'} = \boldsymbol{b}_\perp - \boldsymbol{b}'_\perp$. The perturbative hard factor $\mathcal{H}_{\rm LO}^{\lambda,ij}$ depends on $\boldsymbol{P}_\perp$, Q, and z_i alone; it is specified in the Supplemental Material [47]. The LO WW gluon TMD at the initial projectile-rapidity scale $Y_0 = \ln(z_0)$ is

$$\hat{G}_{Y_0}^{ij}(\boldsymbol{r}_{bb'}, \mu) \equiv \frac{-2}{\alpha_s(\mu)} \left\langle {\rm Tr}\left[V_{\boldsymbol{b}_\perp} \partial^i V_{\boldsymbol{b}_\perp}^\dagger V_{\boldsymbol{b}'_\perp} \partial^j V_{\boldsymbol{b}'_\perp}^\dagger \right] \right\rangle_{Y_0}, \quad (7)$$

where $V_{\boldsymbol{b}_\perp}$ is the lightlike Wilson line in the fundamental representation of SU(3) with transverse coordinate $\boldsymbol{b}_\perp$. The separation of hard versus soft modes (as opposed to fast versus slow) is specified by the renormalization scale μ. In the saturation regime, $\mu \sim Q_s$ since $q_\perp \sim Q_s$ is the typical momentum of the gluon polarization tensor in the shock wave background.

As in the LO case [29,30,48–50], we can extract the NLO impact factor for inclusive back-to-back dijets from the LP contributions ($q_\perp, Q_s \ll P_\perp$) to the fully inclusive

NLO cross section $\langle d\sigma^{\lambda}_{\rm NLO}\rangle_{Y_f}$ [34]. Remarkably, these are also proportional to the WW gluon TMD [22], with dominant contributions to the impact factor from the Sudakov logarithms $\alpha_s\ln^2(P_\perp r_{bb'})$ and $\alpha_s\ln(P_\perp r_{bb'})$ when $P_\perp/q_\perp \gg 1$. The purely $\mathcal{O}(\alpha_s)$ corrections are gathered in the NLO coefficient function. However, in contrast to Eqs. (2) and (4), the LP impact factor at NLO has additional $\ln^2(z_0)$ divergences. They are canceled by imposing a kinematic constraint (kc) in subtracting the $z_g\to 0$ divergence in the back-to-back cross section [51,52],

$$\alpha_s d\sigma^{\lambda,\rm b2b}_{\rm NLO} = \alpha_s\int_0^1\frac{dz_g}{z_g}\int d^2\boldsymbol{z}_\perp\Big[d\tilde{\sigma}^{\lambda,\rm b2b}_{\rm 1L}(z_g,\boldsymbol{z}_\perp) - d\tilde{\sigma}^{\lambda,\rm b2b}_{\rm 1L}(0,\boldsymbol{z}_\perp)\Theta(z_f-z_g)\Theta(-\ln(z_g)-\Delta_c)\Big], \quad (8)$$

where $\Delta_c = \ln(\min(\boldsymbol{r}^2_{zb},\boldsymbol{r}^2_{zb'})2k^+_c q^-)$, $\boldsymbol{r}_{zb} = \boldsymbol{z}_\perp - \boldsymbol{b}_\perp$, $k^+_c = x_c P^+$, and $x_c = (1/ec_0^2)[(M^2_{q\bar{q}}+Q^2)/(W^2+Q^2)]$ is a number fixed in terms of Q^2; W is the nucleon-virtual photon center-of-mass energy, $M_{q\bar{q}} = P_\perp/\sqrt{z_1z_2}$ is the dijet invariant mass, $c_0 = 2e^{-\gamma_E}$, and γ_E is the Euler constant.

Comparing Eq. (8) to Eq. (4), the effect of the kinematic constraint on the LLx RGE in Eq. (5) *specifically* for the WW gluon TMD is to modify the kernel in the JIMWLK Hamiltonian [22,52],

$$H^{kc}_{\rm LL} d\sigma^{\lambda,\rm b2b}_{\rm LO} \equiv \frac{\alpha_s N_c}{2\pi^2}\int_{\boldsymbol{z}_\perp}\Theta(-Y_f-\Delta_c)\mathcal{K}_{\rm LL} d\sigma^{\lambda,\rm b2b}_{\rm LO}. \quad (9)$$

The Θ function enforces lifetime ordering $1/k^+_g \sim 2k^-_g/\boldsymbol{k}^2_\perp \le 1/k^+_c$ in the evolution of the projectile since $1/k^+_c$ is of order of the dipole coherence time $1/|q^+|$ [53,54] and $\boldsymbol{k}^2_\perp \sim 1/\min(\boldsymbol{r}^2_{zb'},\boldsymbol{r}^2_{zb'})$ is the squared transverse momentum of the first emitted gluon. This constraint is long understood [55–65] to generate all-order resummation of transverse double logarithms necessary to match small x with Dokshitzer-Gribov-Lipatov-Altarelli-Parisi collinear resummation. Equation (9) implements a piece of the NLLx RGE; there are additional contributions that require a two-loop computation.

On the surface, Eq. (9) appears process dependent since the kernel depends on the scale k^+_c specific to inclusive back-to-back dijets. This is not the case: replacing Y_f by $\eta_f = \ln(P^+/k^+_f)$ in Eq. (9) using the identity

$$\eta_f = Y_f + \ln\left(\frac{M^2_{q\bar{q}}+Q^2}{eP^2_\perp}\right) + \ln\left(\frac{\boldsymbol{P}^2_\perp\boldsymbol{r}^2_{bb'}}{c_0^2}\right) - \ln(x_c), \quad (10)$$

the Θ constraint in Eq. (9) is replaced by $\eta_f \le \eta_c = \ln(1/x_c)$, the maximal value for the target-rapidity factorization scale η_f. Equation (9) is identical to the universal kinematically constrained dipole RGE in η_f of [66–68] described in the Supplemental Material [47].

Importantly, for scale choice $\eta_f \sim \ln(1/x_c)$, the corresponding scale $Y_f \sim -\ln(\boldsymbol{P}^2_\perp\boldsymbol{r}^2_{bb'})$ in the NLO impact factor is now understood to be a Sudakov log due to gluons with $k^-_f \le k^-_g \lesssim q^-$. The target-rapidity ordered resummation scheme therefore clearly separates small-x rapidity evolution from Sudakov logs (and other NLO corrections) in the NLO impact factor.

The dijet cross section is expanded in Fourier moments as $d\sigma^\lambda = d\sigma^{(0),\lambda} + 2\sum_{n=1}^\infty d\sigma^{(2n),\lambda}\cos(2n\phi)$, where ϕ is the angle between $\boldsymbol{q}_\perp$ and $\boldsymbol{P}_\perp$. At LO, the coefficients of the zeroth and second moment of this expansion are, respectively, proportional to the unpolarized and linearly polarized WW TMD [26–30]. To NLO accuracy, the azimuthally averaged back-to-back dijet cross section has the TMD factorized expression

$$\begin{aligned}\Big\langle d\sigma^{(0),\lambda,\rm b2b}_{\rm LO} + \alpha_s d\sigma^{(0),\lambda,\rm b2b}_{\rm NLO}\Big\rangle_{\eta_f} &= \mathcal{H}^{0,\lambda}_{\rm LO}\int\frac{d^2\boldsymbol{B}_\perp}{(2\pi)^2}\int\frac{d^2\boldsymbol{r}_{bb'}}{(2\pi)^2}e^{-i\boldsymbol{q}_\perp\cdot\boldsymbol{r}_{bb'}}\hat{G}^0_{\eta_f}(\boldsymbol{r}_{bb'},\mu_0)\Bigg\{1 + \frac{\alpha_s(\mu_R)}{\pi}\Bigg[\underbrace{-\frac{N_c}{4}\ln^2\left(\frac{\boldsymbol{P}^2_\perp\boldsymbol{r}^2_{bb'}}{c_0^2}\right)}_{\text{Sudakov double log}} \\ &\quad \underbrace{-s_L\ln\left(\frac{\boldsymbol{P}^2_\perp\boldsymbol{r}^2_{bb'}}{c_0^2}\right) + \beta_0\ln\left(\frac{\mu_R^2\boldsymbol{r}^2_{bb'}}{c_0^2}\right)}_{\text{Sudakov single logs}} + \frac{N_c}{2}f_1^\lambda(\chi,z_1,R,\eta_f) + \frac{1}{2N_c}f_2^\lambda(\chi,z_1,R)\Bigg]\Bigg\} \\ &\quad + \frac{\alpha_s(\mu_R)}{\pi}\mathcal{H}^{0,\lambda}_{\rm LO}\int\frac{d^2\boldsymbol{B}_\perp}{(2\pi)^2}\int\frac{d^2\boldsymbol{r}_{bb'}}{(2\pi)^2}e^{-i\boldsymbol{q}_\perp\cdot\boldsymbol{r}_{bb'}}\hat{h}^0_{\eta_f}(\boldsymbol{r}_{bb'},\mu_0)\left\{\frac{N_c}{2}\left[1+\ln(R^2)\right] - \frac{1}{2N_c}\ln(z_1z_2R^2)\right\}. \end{aligned} \quad (11)$$

Here $\hat{G}^0 = \delta^{ij}\hat{G}^{ij}$ and $\hat{h}^0 = [(2\boldsymbol{r}^i_{bb'}\boldsymbol{r}^j_{bb'}/\boldsymbol{r}^2_{bb'}) - \delta^{ij}]\hat{G}^{ij}$ denote, respectively, the unpolarized and linearly polarized coordinate space WW gluon TMD [69], with both distributions depending implicitly on the impact parameter $\boldsymbol{B}_\perp = \frac{1}{2}(\boldsymbol{b}_\perp + \boldsymbol{b}'_\perp)$. We emphasize that their CGC average is performed at the *target*-rapidity factorization scale $\eta_f = \ln(1/x_f)$. In our numerical study, we shall use $\eta_f = \ln(1/x_g)$ with $x_g = ec_0^2 x_c$ as our central value. A novel feature at NLO is the dependence of Eq. (11) on $\hat{h}^0$. This dependence is absent at LO and arises from soft gluons emitted close to the jet cone boundary [70,71].

Further, in Eq. (11), $\chi \equiv Q/M_{q\bar{q}}$ and R is the anti-k_t jet radius [72]. The coefficient of the single Sudakov logarithm is $s_L = -C_F \ln(z_1 z_2 R^2) + N_c \ln(1+\chi^2)$. The term proportional to the coefficient $\beta_0 = (11N_c - 2n_f)/12$ of the one-loop β function arises from the renormalization group (RG) evolution of the WW TMD as a function of μ from the initial scale $\mu_0^2 = c_0^2/\boldsymbol{r}_{bb'}^2$ up to the renormalization scale μ_R^2 [22,73,74]. Since $\mu_R \sim P_\perp$, this term can be combined with the Sudakov single logarithm. The NLO coefficient functions f_1 and f_2 have analytic expressions specified in the Supplemental Material [47] (including Refs. [75–83]).

Equation (11) is the principal result of this Letter. It demonstrates for the first time TMD factorization of the back-to-back dijet cross section at small x at NLO. It is valid up to corrections of order $q_\perp^2/P_\perp^2$ and $Q_s^2/P_\perp^2$, as well as $\alpha_s R^2$ and α_s^2. All saturation effects are contained in the WW gluon TMD $\hat{G}^{ij}_{\eta_f}$ and its nonlinear kinematically constrained RGE, without introducing new operators in the NLO coefficient functions. Although TMD factorization could have been anticipated for $q_\perp \gg Q_s$ since the high-energy evolution equation of the WW gluon TMD has a closed form in this dilute limit [84], it is remarkable that it persists when $q_\perp \sim Q_s$, enabling precise extraction of saturation dynamics with back-to-back dijets. Explicit expressions for higher-order even harmonics $d\sigma^{(2n),\lambda}$ are provided in the Supplemental Material [47].

In Eq. (11), we obtained the $\mathcal{O}(\alpha_s)$ term for Sudakov logs for this process at small x. If we assume powers of these logarithms at all orders can be resummed and exponentiate [85–87], as in the Collins-Soper-Sterman collinear factorization framework [88–90], they can be absorbed in a Sudakov soft factor

$$\mathcal{S} = \exp\left(-\int_{\mu_0^2}^{P_\perp^2} \frac{d\mu^2}{\mu^2} \frac{\alpha_s N_c}{\pi}\left[\frac{1}{2}\ln\left(\frac{P_\perp^2}{\mu^2}\right) + \frac{\tilde{s}_L}{N_c}\right]\right). \quad (12)$$

Here $\tilde{s}_L = s_L - \beta_0$ and $\alpha_s = \alpha_s(c\mu)$, where c is an arbitrary $\mathcal{O}(1)$ constant that can be varied to gauge the sensitivity to two-loop $\mathcal{O}[\alpha_s^2 \ln^2(P_\perp/\mu_0)]$ corrections not included in the resummation [90]. The Sudakov factor agrees with previous collinear factorization calculations for this process [71]. This is noteworthy given the nontrivial interplay between Sudakov and small-x factorization. The result of the resummation (shown in the Supplemental Material [47]) is to remove the underlined Sudakov log terms in Eq. (11) and multiply instead the WW TMD by $\mathcal{S}$.

We shall now discuss the numerical evaluation of Eq. (11) and higher Fourier moments to assess their predictive power at the EIC. We compute the differential yield $dN = \Sigma_\lambda \phi^\lambda d\sigma^\lambda/d^2\boldsymbol{B}_\perp$ at the mean impact parameter, which represents minimum bias collisions. (ϕ^λ is the photon flux factor defined in the Supplemental Material [47].) For $\sqrt{s} = 90$ GeV, $Q^2 = 4$ GeV^2, and $x_{\rm Bj} = 0.55 \times 10^{-3}$, the smallest x available for RG evolution is $x_c = (1.5 - 3.8) \times 10^{-3}$ for $P_\perp = (4–6)$ GeV. While not a large window, we will demonstrate that it may be sufficient to uncover clear evidence for gluon saturation.

Using the Gaussian approximation [69,91–94], we first relate the WW gluon TMD to the dipole gluon distribution $\mathcal{N}_{\eta_f}(\boldsymbol{r}_\perp)$ satisfying the Balitsky-Kovchegov (BK) RGE [35,95,96]. For the initial condition for the RGE, we use the McLerran-Venugopalan model [2,3],

$$\mathcal{N}_{\eta_0}(\boldsymbol{r}_\perp) = 1 - \exp\left[-\frac{\boldsymbol{r}_\perp^2 Q_{s0,A}^2}{4}\ln\left(\frac{1}{r_\perp \Lambda} + e\right)\right], \quad (13)$$

with the rapidity scale $\eta_0 = \ln(1/x_0)$, $x_0 = 2.5 \times 10^{-2}$, and the minimum bias $Q_{s0,A}^2 = A^{1/3} \times 0.1$ GeV^2 [97]. The infrared regulator of the Coulomb logarithm is $\Lambda = 0.24$ GeV. Fits to $e + A$ fixed target data [98] and electron-proton ($e + p$) HERA data [99] dictate these choices, which can be constrained from future global analyses.

For full NLO accuracy at small x, one should evolve $\mathcal{N}_{\eta_0}(\boldsymbol{r}_\perp)$ with the NLLx BK equation [100]. While this equation is challenging to solve [101], the dominant contributions to its kernel are accounted for by contributions from the running coupling and the lifetime ordering constraint [102]. We employ the minimal dipole size prescription for the former [100,103,104]. For the Sudakov soft factor in Eq. (12), we employ one-loop running of the coupling. Its sensitivity to nonperturbative physics at large $r_{bb'}$ is modeled by freezing it at a maximal value (which is varied) of $\alpha_{s,\max}/\pi = 0.24$.

Results in EIC kinematics for the azimuthally averaged back-to-back dijet yield versus $q_\perp$ are shown in Fig. 2 (top). It illustrates the effects of three types of NLO corrections: (i) Sudakov suppression (green dashed curve), (ii) Sudakov suppression and small-x evolution (dot-dashed blue curve), and (iii) all NLO corrections labeled NLO (full)—this includes as well the NLO coefficient function computed for the first time here. In comparing the dotted red and dashed green curves, one observes that Sudakov suppression is very significant for $q_\perp \lesssim 1.5$ GeV. Small-x resummation leads to an overall increase of the yield due to the proliferation of slow gluons. This increase is slowed down by nonlinear saturation corrections. The NLO coefficient function yields a small additional contribution to the yield, which varies depending on kinematic choices. The light green band shows the dependence of the full NLO result on the jet radius R, which decreases slightly with increasing R.

The inset shows the $q_\perp$ dependence of the $v_2 = d\sigma^{(2)}/d\sigma^{(0)}$ coefficient, whose magnitude is very small, $< 2\%$. NLO corrections on the sign of v_2 are significant because they flip the LO (negative) value due to the preferential emission of soft gluons close to the jet boundary. The sign of v_2 is therefore sensitive to R; however, as shown in the Supplemental Material [47],

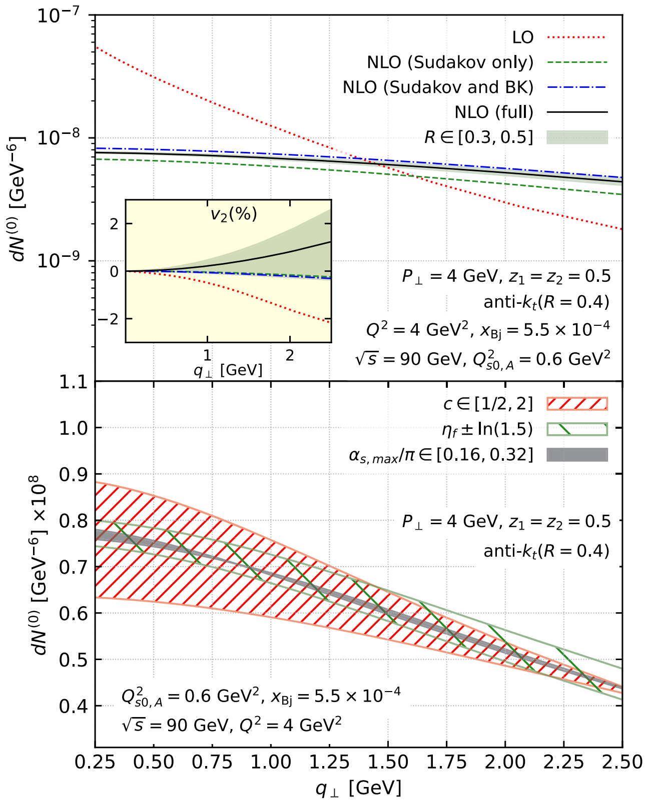

FIG. 2. Top: azimuthally averaged LO and NLO back-to-back dijet yield as a function of dijet momentum imbalance $q_\perp$. Inset: $q_\perp$ dependence of the v_2 coefficient. The light green band corresponds to varying anti-k_t parameter $R = 0.3$–0.5. Bottom: theory uncertainties from renormalization and target-rapidity scale variations and freezing of α_s. Details in text.

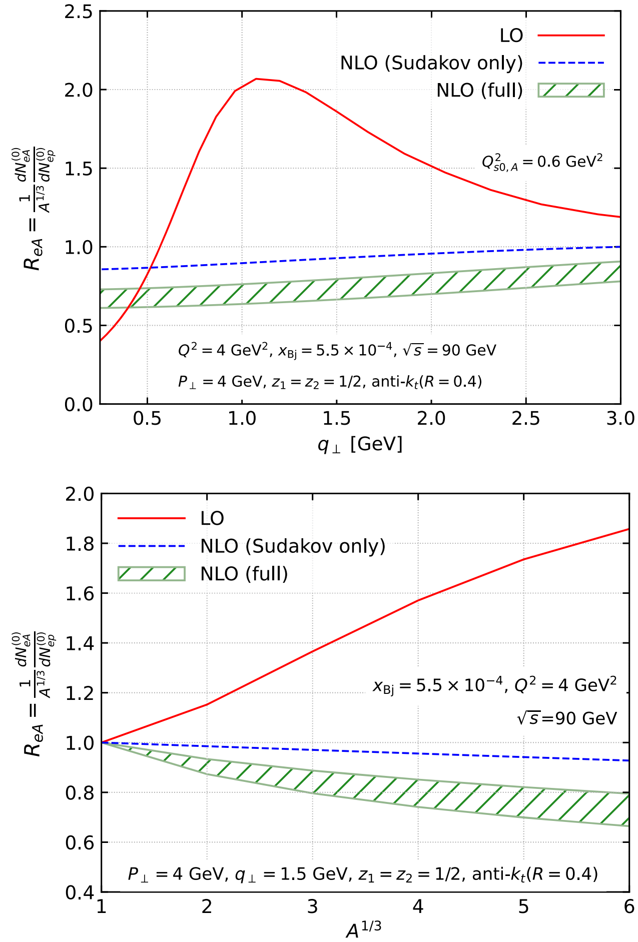

FIG. 3. $q_\perp$ and A dependence (top and bottom, respectively) of the nuclear modification factor R_{eA} for the azimuthally averaged back-to-back dijet yield.

$v_2^{\lambda=L} \propto \hat{h}^0$ is unambiguously positive for the R range studied.

Theory uncertainties in the NLO result can be divided into four classes; three of these are displayed in Fig. 2 (bottom). We first show uncertainties from the unknown order N^{2}LO contributions beyond the NLO impact factor; they are estimated by varying the running coupling scale $c = 0.5$–2 both in the NLO coefficient function where $\mu_R = cP_\perp$ and in the Sudakov factor. Since they are parametrically of order $\alpha_s^2 \ln^2(P_\perp/\mu_0)$, the band width grows with decreasing $q_\perp$. This illustrates the importance of controlling powers of $\alpha_s \ln(P_\perp/\mu_0)$ for future precision studies.

The second source of uncertainty is from the target-rapidity factorization scale η_f, obtained by varying x_f by a factor of 1.5 around the central value x_g. This dependence decreases from LO to NLO (see Supplemental Material [47]); it remains, however, the dominant source of uncertainty for $q_\perp \gtrsim Q_s$. Uncertainties from missing contributions in the full NLL BK kernel are subleading in comparison. Variations with respect to $\alpha_{s,\max}$ are shown by the gray band in Fig. 2 (bottom). This sensitivity is mitigated in large nuclei because the minimal transverse size controlling the coupling is set by the large Q_s. Not shown here are power correction $(q_\perp^2/P_\perp^2, Q_s^2/P_\perp^2)$ uncertainties discussed at LO in [29,30], of $\mathcal{O}(10\%)$ for $q_\perp \lesssim 1.5$ and $P_\perp = 4$ GeV.

Figure 3 displays R_{eA}, the ratio of the azimuthally averaged back-to-back dijet yield in $e + A$ to $e + p$ collisions. Such ratios minimize theory uncertainties as well as experimental ones. The top plot shows the $q_\perp$ dependence of R_{eA} for a large nucleus; for simplicity, we take $A^{1/3} = 6$. At LO, it has a "Cronin" peak, well known from the corresponding ratio in proton-nucleus ($p + A$) collisions [105]; in the CGC, it is generated by coherent multiple scattering that shifts the typical momentum imbalance to larger $q_\perp$ in heavier nuclei [106]. At NLO, we see that the Cronin enhancement is washed out by Sudakov corrections alone. A further strong effect is seen from the NLO contributions dominantly caused by the WW gluon TMD RGE, which suppresses R_{eA} as in the R_{pA} case [107,108].

A qualitative interpretation is that Sudakov logs suppress configurations corresponding to small $q_\perp$ (or large $\boldsymbol{r}_{bb'}$) in the projectile. However, since a fundamental consequence of gluon saturation is that even configurations with small $\boldsymbol{r}_{bb'}$ are sensitive to nonlinear RG x evolution, its precocious onset in large nuclei [109] leads to increasing suppression of R_{eA} with $A^{1/3}$, as demonstrated by the bottom plot for fixed $q_\perp = 1.5$ GeV. The systematics of this suppression with $A^{1/3}$ and $q_\perp$ are sensitive to the WW TMD RGE. Plots with different kinematic choices are provided in the Supplemental Material [47].

While more detailed studies are necessary, our results are suggestive that inclusive back-to-back dijets in $e + A$ collisions show strong potential to be a golden channel for gluon saturation at the EIC when combined with other processes that constrain the initial condition for the WW small-x RGE. Our conclusions can be strengthened by minimizing the stated theory uncertainties and by extending the comprehensive NLO study here to the dihadron channel. Global analyses incorporating other $e + A$ small-x final states [110–121] and analogous studies [122–138] in $p + A$ collisions at the Relativistic Heavy Ion Collider and the LHC will further enable unambiguous determination of the dynamics of gluon saturation.

We are grateful to Bertrand Ducloué and Feng Yuan for valuable discussions. P. C., F. S., and T. S. thank the EIC theory institute at BNL for its support during the final stages of this work. F. S. is supported by the National Science Foundation, under Grant No. PHY-1945471, and the UC Southern California hub, with funding from the UC National Laboratories division of the University of California Office of the President. T. S. kindly acknowledges support of the Polish National Science Center (NCN) Grants No. 2019/32/C/ST2/00202 and No. 2021/43/D/ST2/03375. B. P. S. and R. V. are supported by the U.S. Department of Energy, Office of Science, Office of Nuclear Physics, under DOE Award No. DE-SC0012704 and within the framework of the Saturated Glue (SURGE) Topical Theory Collaboration. R. V.'s work is also supported in part by an LDRD grant from Brookhaven Science Associates.

[*]caucal@subatech.in2p3.fr
[†]salazar@lbl.gov
[‡]bschenke@bnl.gov
[§]tomasz.stebel@uj.edu.pl
[‖]raju@bnl.gov

[1] R. Boussarie *et al.*, arXiv:2304.03302.
[2] L. D. McLerran and R. Venugopalan, Phys. Rev. D **49**, 2233 (1994).
[3] L. D. McLerran and R. Venugopalan, Phys. Rev. D **49**, 3352 (1994).
[4] Y. V. Kovchegov and A. H. Mueller, Nucl. Phys. **B529**, 451 (1998).
[5] L. Gribov, E. Levin, and M. Ryskin, Phys. Rep. **100**, 1 (1983).
[6] A. H. Mueller and J.-w. Qiu, Nucl. Phys. **B268**, 427 (1986).
[7] F. Dominguez, B.-W. Xiao, and F. Yuan, Phys. Rev. Lett. **106**, 022301 (2011).
[8] F. Dominguez, C. Marquet, B.-W. Xiao, and F. Yuan, Phys. Rev. D **83**, 105005 (2011).
[9] S. Catani and L. Trentadue, Nucl. Phys. **B327**, 323 (1989).
[10] S. Catani and L. Trentadue, Nucl. Phys. **B353**, 183 (1991).
[11] S. Catani and F. Hautmann, Nucl. Phys. **B427**, 475 (1994).
[12] I. Balitsky and A. Tarasov, J. High Energy Phys. 10 (2015) 017.
[13] I. Balitsky and G. A. Chirilli, Phys. Rev. D **106**, 034007 (2022).
[14] I. Balitsky, J. High Energy Phys. 03 (2023) 029.
[15] A. H. Mueller, B.-W. Xiao, and F. Yuan, Phys. Rev. Lett. **110**, 082301 (2013).
[16] A. H. Mueller, B.-W. Xiao, and F. Yuan, Phys. Rev. D **88**, 114010 (2013).
[17] B.-W. Xiao, F. Yuan, and J. Zhou, Nucl. Phys. **B921**, 104 (2017).
[18] F. Gelis and J. Jalilian-Marian, Phys. Rev. D **67**, 074019 (2003).
[19] J. L. Albacete and C. Marquet, Prog. Part. Nucl. Phys. **76**, 1 (2014).
[20] A. Morreale and F. Salazar, Universe **7**, 312 (2021).
[21] A detailed derivation of the cross section for longitudinally polarized virtual photons is provided in a previous paper [22].
[22] P. Caucal, F. Salazar, B. Schenke, T. Stebel, and R. Venugopalan, J. High Energy Phys. 08 (2023) 062.
[23] A. Accardi *et al.*, Eur. Phys. J. A **52**, 268 (2016).
[24] E. C. Aschenauer, S. Fazio, J. H. Lee, H. Mäntysaari, B. S. Page, B. Schenke, T. Ullrich, R. Venugopalan, and P. Zurita, Rep. Prog. Phys. **82**, 024301 (2019).
[25] R. Abdul Khalek *et al.*, Nucl. Phys. **A1026**, 122447 (2022).
[26] A. Dumitru and V. Skokov, Phys. Rev. D **91**, 074006 (2015).
[27] A. Dumitru, V. Skokov, and T. Ullrich, Phys. Rev. C **99**, 015204 (2019).
[28] Y.-Y. Zhao, M.-M. Xu, L.-Z. Chen, D.-H. Zhang, and Y.-F. Wu, Phys. Rev. D **104**, 114032 (2021).
[29] H. Mäntysaari, N. Mueller, F. Salazar, and B. Schenke, Phys. Rev. Lett. **124**, 112301 (2020).
[30] R. Boussarie, H. Mäntysaari, F. Salazar, and B. Schenke, J. High Energy Phys. 09 (**2021**) 178.
[31] A. van Hameren, P. Kotko, K. Kutak, S. Sapeta, and E. Żarów, Eur. Phys. J. C **81**, 741 (2021).
[32] L. Zheng, E. C. Aschenauer, J. H. Lee, and B.-W. Xiao, Proc. Sci., DIS2014 (**2014**) 255.
[33] F. Bergabo and J. Jalilian-Marian, Phys. Rev. D **107**, 054036 (2023).
[34] P. Caucal, F. Salazar, and R. Venugopalan, J. High Energy Phys. 11 (2021) 222.
[35] I. Balitsky, Nucl. Phys. **B463**, 99 (1996).
[36] J. Jalilian-Marian, A. Kovner, L. D. McLerran, and H. Weigert, Phys. Rev. D **55**, 5414 (1997).
[37] J. Jalilian-Marian, A. Kovner, and H. Weigert, Phys. Rev. D **59**, 014015 (1998).
[38] A. Kovner, J. G. Milhano, and H. Weigert, Phys. Rev. D **62**, 114005 (2000).
[39] E. Iancu, A. Leonidov, and L. D. McLerran, Nucl. Phys. **A692**, 583 (2001).
[40] E. Iancu, A. Leonidov, and L. D. McLerran, Phys. Lett. B **510**, 133 (2001).

[41] E. Ferreiro, E. Iancu, A. Leonidov, and L. McLerran, Nucl. Phys. **A703**, 489 (2002).

[42] We use the words projectile rapidity for $Y = \ln(k^-/q^-)$ and target rapidity for $\eta = \ln(P^+/k^+)$. These two scales are related to the physical rapidity $y = 1/2\ln(k^+/k^-)$ via the kinematic identity $y = y_{\gamma^*} - 1/2[\ln(x_{\mathrm{Bj}}) + Y + \eta]$ where y_{γ^*} is the rapidity of the virtual photon.

[43] I. Balitsky and G. A. Chirilli, Phys. Rev. D **88**, 111501(R) (2013).

[44] A. Kovner, M. Lublinsky, and Y. Mulian, Phys. Rev. D **89**, 061704(R) (2014).

[45] A. Kovner, M. Lublinsky, and Y. Mulian, J. High Energy Phys. 08 (2014) 114.

[46] M. Lublinsky and Y. Mulian, J. High Energy Phys. 05 (2017) 097.

[47] See Supplemental Material at http://link.aps.org/supplemental/10.1103/PhysRevLett.132.081902 for the analytic expressions of the NLO coefficient functions, additional plots, a discussion of the kinematically constrained RGE of the WW gluon TMD and further details on the calculation of the NLO hard factors.

[48] T. Altinoluk and R. Boussarie, J. High Energy Phys. 10 (2019) 208.

[49] R. Boussarie and Y. Mehtar-Tani, Phys. Rev. D **103**, 094012 (2021).

[50] B. Rodriguez-Aguilar, D. N. Triantafyllopoulos, and S. Y. Wei, Phys. Rev. D **107**, 114007 (2023).

[51] P. Caucal, F. Salazar, B. Schenke, and R. Venugopalan, J. High Energy Phys. 11 (**2022**) 169.

[52] P. Taels, T. Altinoluk, G. Beuf, and C. Marquet, J. High Energy Phys. 10 (2022) 184.

[53] V. N. Gribov, B. L. Ioffe, and I. Y. Pomeranchuk, Yad. Fiz. **2**, 768 (1965).

[54] B. L. Ioffe, Phys. Lett. **30B**, 123 (1969).

[55] B. Andersson, G. Gustafson, and J. Samuelsson, Nucl. Phys. **B467**, 443 (1996).

[56] J. Kwiecinski, A. D. Martin, and P. J. Sutton, Z. Phys. C **71**, 585 (1996).

[57] J. Kwiecinski, A. D. Martin, and A. M. Stasto, Phys. Rev. D **56**, 3991 (1997).

[58] G. P. Salam, J. High Energy Phys. 07 (1998) 019.

[59] M. Ciafaloni and D. Colferai, Phys. Lett. B **452**, 372 (1999).

[60] M. Ciafaloni, D. Colferai, and G. P. Salam, Phys. Rev. D **60**, 114036 (1999).

[61] M. Ciafaloni, D. Colferai, G. P. Salam, and A. M. Stasto, Phys. Rev. D **68**, 114003 (2003).

[62] A. Sabio Vera, Nucl. Phys. **B722**, 65 (2005).

[63] L. Motyka and A. M. Stasto, Phys. Rev. D **79**, 085016 (2009).

[64] G. Beuf, Phys. Rev. D **89**, 074039 (2014).

[65] E. Iancu, J. Madrigal, A. Mueller, G. Soyez, and D. Triantafyllopoulos, Phys. Lett. B **744**, 293 (2015).

[66] Y. Hatta and E. Iancu, J. High Energy Phys. 08 (2016) 083.

[67] B. Ducloué, E. Iancu, A. Mueller, G. Soyez, and D. Triantafyllopoulos, J. High Energy Phys. 04 (2019) 081.

[68] B. Ducloué, E. Iancu, G. Soyez, and D. N. Triantafyllopoulos, Phys. Lett. B **803**, 135305 (2020).

[69] F. Dominguez, J.-W. Qiu, B.-W. Xiao, and F. Yuan, Phys. Rev. D **85**, 045003 (2012).

[70] Y. Hatta, B.-W. Xiao, F. Yuan, and J. Zhou, Phys. Rev. Lett. **126**, 142001 (2021).

[71] Y. Hatta, B.-W. Xiao, F. Yuan, and J. Zhou, Phys. Rev. D **104**, 054037 (2021).

[72] M. Cacciari, G. P. Salam, and G. Soyez, J. High Energy Phys. 04 (2008) 063.

[73] A. Ayala, J. Jalilian-Marian, L. D. McLerran, and R. Venugopalan, Phys. Rev. D **53**, 458 (1996).

[74] J. Zhou, Phys. Rev. D **99**, 054026 (2019).

[75] Y. L. Dokshitzer, G. D. Leder, S. Moretti, and B. R. Webber, J. High Energy Phys. 08 (1997) 001.

[76] M. Wobisch and T. Wengler, in *Proceedings of the Workshop on Monte Carlo Generators for HERA Physics (Plenary Starting Meeting)* (1998), pp. 270–279; arXiv:hep-ph/9907280.

[77] G. P. Salam, Eur. Phys. J. C **67**, 637 (2010).

[78] M. Cacciari, G. P. Salam, and G. Soyez, Eur. Phys. J. C **72**, 1896 (2012).

[79] G. P. Salam and G. Soyez, J. High Energy Phys. 05 (2007) 086.

[80] D. Y. Ivanov and A. Papa, J. High Energy Phys. 05 (2012) 086.

[81] Z.-B. Kang, F. Ringer, and W. J. Waalewijn, J. High Energy Phys. 07 (2017) 064.

[82] M. Abramowitz and I. A. Stegun, *Handbook of Mathematical Functions with Formulas, Graphs, and Mathematical Tables* (U.S. GPO, Washington, DC, 1964), Vol. 55.

[83] S. Cali, K. Cichy, P. Korcyl, P. Kotko, K. Kutak, and C. Marquet, Eur. Phys. J. C **81**, 663 (2021).

[84] F. Dominguez, A. H. Mueller, S. Munier, and B.-W. Xiao, Phys. Lett. B **705**, 106 (2011).

[85] Z.-B. Kang, J. Reiten, D. Y. Shao, and J. Terry, J. High Energy Phys. 05 (2021) 286.

[86] R. F. del Castillo, M. G. Echevarria, Y. Makris, and I. Scimemi, J. High Energy Phys. 01 (2021) 088.

[87] M.-S. Gao, Z.-B. Kang, D. Y. Shao, J. Terry, and C. Zhang, J. High Energy Phys. 10 (2023) 013.

[88] J. C. Collins and D. E. Soper, Nucl. Phys. **B193**, 381 (1981); **B213**, 545(E) (1983).

[89] J. C. Collins and D. E. Soper, Nucl. Phys. **B194**, 445 (1982).

[90] J. C. Collins, D. E. Soper, and G. F. Sterman, Nucl. Phys. **B250**, 199 (1985).

[91] J. P. Blaizot, F. Gelis, and R. Venugopalan, Nucl. Phys. **A743**, 57 (2004).

[92] A. Dumitru, J. Jalilian-Marian, T. Lappi, B. Schenke, and R. Venugopalan, Phys. Lett. B **706**, 219 (2011).

[93] E. Iancu and D. N. Triantafyllopoulos, J. High Energy Phys. 04 (2012) 025.

[94] A. Metz and J. Zhou, Phys. Rev. D **84**, 051503(R) (2011).

[95] Y. V. Kovchegov, Phys. Rev. D **60**, 034008 (1999).

[96] The validity of this approximation relative to the full LL JIMWLK RGE was explored in [92] and shown to be quite good for a range of spatial configurations of dipoles.

[97] H. Kowalski, T. Lappi, and R. Venugopalan, Phys. Rev. Lett. **100**, 022303 (2008).

[98] T. Lappi and H. Mäntysaari, Phys. Rev. D **88**, 114020 (2013).

[99] F. D. Aaron *et al.* (H1 and ZEUS Collaborations), J. High Energy Phys. 01 (2010) 109.
[100] I. Balitsky and G. A. Chirilli, Phys. Rev. D **77**, 014019 (2008).
[101] T. Lappi and H. Mäntysaari, Phys. Rev. D **91**, 074016 (2015).
[102] T. Lappi and H. Mäntysaari, Phys. Rev. D **93**, 094004 (2016).
[103] Y. V. Kovchegov and H. Weigert, Nucl. Phys. **A784**, 188 (2007).
[104] E. Iancu, J. D. Madrigal, A. H. Mueller, G. Soyez, and D. N. Triantafyllopoulos, Phys. Lett. B **750**, 643 (2015).
[105] D. Antreasyan, J. W. Cronin, H. J. Frisch, M. J. Shochet, L. Kluberg, P. A. Piroue, and R. L. Sumner, Phys. Rev. D **19**, 764 (1979).
[106] J. Jalilian-Marian, Y. Nara, and R. Venugopalan, Phys. Lett. B **577**, 54 (2003).
[107] D. Kharzeev, Y. V. Kovchegov, and K. Tuchin, Phys. Rev. D **68**, 094013 (2003).
[108] J. L. Albacete, N. Armesto, A. Kovner, C. A. Salgado, and U. A. Wiedemann, Phys. Rev. Lett. **92**, 082001 (2004).
[109] A. H. Mueller, Nucl. Phys. **A724**, 223 (2003).
[110] R. Boussarie, A. V. Grabovsky, D. Yu. Ivanov, L. Szymanowski, and S. Wallon, Phys. Rev. Lett. **119**, 072002 (2017).
[111] R. Boussarie, A. V. Grabovsky, L. Szymanowski, and S. Wallon, J. High Energy Phys. 11 (2016) 149.
[112] K. Roy and R. Venugopalan, Phys. Rev. D **101**, 071505(R) (2020).
[113] K. Roy and R. Venugopalan, Phys. Rev. D **101**, 034028 (2020).
[114] G. Beuf, H. Hänninen, T. Lappi, and H. Mäntysaari, Phys. Rev. D **102**, 074028 (2020).
[115] G. Beuf, T. Lappi, and R. Paatelainen, Phys. Rev. Lett. **129**, 072001 (2022).
[116] H. Mäntysaari and J. Penttala, J. High Energy Phys. 08 (2022) 247.
[117] F. Bergabo and J. Jalilian-Marian, J. High Energy Phys. 01 (2023) 095.
[118] G. Beuf, H. Hänninen, T. Lappi, Y. Mulian, and H. Mäntysaari, Phys. Rev. D **106**, 094014 (2022).
[119] X.-B. Tong, B.-W. Xiao, and Y.-Y. Zhang, Phys. Rev. Lett. **130**, 151902 (2023).
[120] M. Fucilla, A. V. Grabovsky, E. Li, L. Szymanowski, and S. Wallon, J. High Energy Phys. 03 (2023) 159.
[121] A. V. Lipatov and M. A. Malyshev, Phys. Rev. D **108**, 014022 (2023).
[122] G. A. Chirilli, B.-W. Xiao, and F. Yuan, Phys. Rev. Lett. **108**, 122301 (2012).
[123] D. Y. Ivanov and A. Papa, J. High Energy Phys. 07 (2012) 045.
[124] T. Altinoluk, N. Armesto, G. Beuf, A. Kovner, and M. Lublinsky, Phys. Rev. D **91**, 094016 (2015).
[125] F. G. Celiberto, D. Y. Ivanov, B. Murdaca, and A. Papa, Eur. Phys. J. C **77**, 382 (2017).
[126] A. Stasto, S.-Y. Wei, B.-W. Xiao, and F. Yuan, Phys. Lett. B **784**, 301 (2018).
[127] J. L. Albacete, G. Giacalone, C. Marquet, and M. Matas, Phys. Rev. D **99**, 014002 (2019).
[128] H.-Y. Liu, Z.-B. Kang, and X. Liu, Phys. Rev. D **102**, 051502(R) (2020).
[129] Y. Shi, L. Wang, S.-Y. Wei, and B.-W. Xiao, Phys. Rev. Lett. **128**, 202302 (2022).
[130] M. Hentschinski, Phys. Rev. D **104**, 054014 (2021).
[131] H.-y. Liu, K. Xie, Z. Kang, and X. Liu, J. High Energy Phys. 07 (2022) 041.
[132] L. Wang, L. Chen, Z. Gao, Y. Shi, S.-Y. Wei, and B.-W. Xiao, Phys. Rev. D **107**, 016016 (2023).
[133] A. van Hameren, L. Motyka, and G. Ziarko, J. High Energy Phys. 11 (2022) 103.
[134] M. Hentschinski, K. Kutak, and A. van Hameren, Eur. Phys. J. C **81**, 112 (2021); **81**, 262(E) (2021).
[135] F. G. Celiberto, M. Fucilla, D. Y. Ivanov, M. M. A. Mohammed, and A. Papa, J. High Energy Phys. 08 (2022) 092.
[136] A. van Hameren, H. Kakkad, P. Kotko, K. Kutak, and S. Sapeta, Eur. Phys. J. C **83**, 947 (2023).
[137] I. Ganguli, A. van Hameren, P. Kotko, and K. Kutak, Eur. Phys. J. C **83**, 868 (2023).
[138] T. Altinoluk, N. Armesto, A. Kovner, and M. Lublinsky, Phys. Rev. D **108**, 074003 (2023).